CHEMBIOCHEM

DOI: 10.1002/cbic.200700457

The Identification and Characterization of Fusogenic Domains in Herpes Virus Glycoprotein B Molecules

Stefania Galdiero,[a, b, c] Mariateresa Vitiello,[d] Marina D'Isanto,[d] Annarita Falanga,[d] Marco Cantisani,[a, b, c] Helena Browne,[e] Carlo Pedone,[a, b, c] and Massimiliano Galdiero*[b, d]

The molecular mechanism of entry of herpes viruses requires a multicomponent fusion system. Virus entry and cell–cell fusion of Herpes simplex *virus (HSV) requires four glycoproteins: gD, gB and gH/gL. The role of gB remained elusive until recently, when the crystal structure of HSV-1 gB became available. Glycoprotein B homologues represent the most highly conserved group of herpes virus glycoproteins; however, despite the high degree of sequence and structural conservation, differences in post-translational processing are observed for different members of this virus family. Whereas gB of HSV is not proteolytically processed after oligomerization, most other gB homologues are cleaved by a cellular protease into subunits that remain linked through disulfide bonds. Proteolytic cleavage is common for activation of many other viral fusion proteins, so it remains difficult to envisage a common role for different herpes virus gB structures in the fusion mechanism. We selected bovine herpes virus type 1 (BoHV-1) and* herpes simplex *virus type 1 (HSV-1) as representative viruses expressing cleaved and uncleaved gBs, and have screened their amino acid sequences for regions of highly interfacial hydrophobicity. Synthetic peptides corresponding to such regions were tested for their ability to induce the fusion of large unilamellar vesicles and to inhibit herpes virus infection. These results underline that several regions of the gB protein are involved in the mechanism of membrane interaction.*

Introduction

Herpes simplex virus (HSV) enters cells through fusion of the virus envelope with a cellular membrane in a cascade of molecular interactions involving multiple viral glycoproteins and cellular receptors. The envelope glycoproteins gH/gL, gB and gD are all essential for the entry process,[1–3] and expression of this quartet of glycoproteins induces the fusion of cellular membranes in the absence of virus infection.[4]

The first contact of the virus with the cell is mediated by glycoprotein C (gC), which interacts with cell surface proteoglycans,[5] and this process is followed by a more specific interaction of gD with one of a number of different cellular receptors, including nectin-1, an intercellular adhesion molecule, and herpes virus entry mediator (HVEM), a member of the tumour necrosis factor α receptor family.[6,7]

The crystal structure of the soluble ectodomain of gD[8,9] shows that binding of gD and the receptor promotes a conformational change in gD whereby its C-terminal segment is released from strong intramolecular constraints. It has been proposed that this conformational change in gD results in subsequent fusion induction, mediated by gB and/or gH/gL.[9]

There are also reports that fusion is mediated through a hemifusion intermediate involving direct interactions of gH/gL and gB with the cell membrane.[10]

Although gH and gB are the main candidate proteins for performing fusion, their mechanisms of function are still unknown. It was recently reported that gH possesses several hydrophobic domains necessary for efficient induction of fusion;[11,12] moreover, gH also contains two heptad repeat (HR) domains, and peptides corresponding to these regions inhibit HSV-1 infection.[13,14]

gB homologues are highly conserved within the herpes virus family, and this glycoprotein is involved in virus attachment, penetration and cell-to-cell spread.[3,15–18]

The HSV-1 gB gene encodes 904 amino acids.[19] Biochemical analysis has shown that it contains a 30-residue N-terminal signal sequence that is cleaved during processing, a 743-residue external domain, a 22-residue transmembrane domain and a 109-residue cytoplasmic domain.[19–21]

The crystal structure of HSV-1 gB has been solved at a resolution of 2.1 Å[22] and revealed that gB is present as a trimeric spike with approximate dimensions of $85 \times 80 \times 160$ Å. The bulk of each unit coils around the others with a left-handed twist

[a] *Dr. S. Galdiero,[+] Dr. M. Cantisani, Prof. C. Pedone*
Department of Biological Sciences, Division of Biostructures
University of Naples "Federico II"
Via Mezzocannone 16, 80134 Napoli (Italy)

[b] *Dr. S. Galdiero,[+] Dr. M. Cantisani, Prof. C. Pedone, Prof. M. Galdiero*
Centro Interuniversitario di Ricerca sui Peptidi Bioattivi
University of Naples "Federico II"
Via Mezzocannone 16, 80134 Napoli (Italy)

[c] *Dr. S. Galdiero,[+] Dr. M. Cantisani, Prof. C. Pedone*
Istituto di Biostrutture e Bioimmagini CNR
Via Mezzocannone 16, 80134 Napoli (Italy)

[d] *Dr. M. Vitiello,[+] Dr. M. D'Isanto, Dr. A. Falanga, Prof. M. Galdiero*
Department of Experimental Medicine II University of Naples
Via De Crecchio 7, 80138 Napoli (Italy)
Fax: (+39) 081-5667578
E-mail: massimiliano.galdiero@unina2.it

[e] *Dr. H. Browne*
Division of Virology, Department of Pathology, University of Cambridge
Tennis Court Road, CB2 1QP Cambridge (UK)

[+] *These authors contributed equally to this work.*

and there is no trimerization domain per se; instead, multiple contacts between subunits throughout the molecule contribute to trimer stability. The gB homologues of a number of different herpes viruses contain the sequence motif RXK/RR, which is the recognition site for proteolytic cleavage by the cellular endoprotease furin. Such viruses include varicella-zoster virus, bovine herpes virus type 1 (BoHV-1), pseudorabies virus (PRV), equine herpes virus, Marek's disease virus and all known β-herpes viruses, including human cytomegalovirus (HCMV) and human herpes virus 6.[23–29] In contrast, other herpes viruses—such as Epstein–Barr virus, HSV-1 and HSV-2 and simian herpes virus B—express gB molecules that lack a furin cleavage site.[30,31] Studies of BoHV-1 and PRV have shown that if the cleavage site in gB is mutated to a noncleavable form, virion infectivity is unaffected, even though the resulting plaques were significantly smaller in size, indicating a role for proteolytic cleavage of BoHV-1 in cell-to-cell spread.[32] It has also been shown that PRV gB (which is proteolytically processed) can complement an HSV gB-null mutant, but that the uncleaved HSV-1 gB cannot rescue the infectivity of a PRV gB-null virus.[33] Furthermore, viruses with mutations in the furin cleavage site of HCMV gB were fully replication-competent.[34] These observations suggest that herpes virus gB homologues, despite their structural conservation, carry out additional unique functions within their respective viral contexts.

Proteolytic processing is generally required for activation of the fusogenic properties of many viral class I fusion glycoproteins. The cleavage process produces two subunits: one is anchored to the viral envelope through a transmembrane domain and bears a hydrophobic region that serves as a fusion peptide at its N terminus, while the other subunit interacts with a cell surface receptor and usually remains associated to the first subunit through disulfide bonds.

Since gB is cleaved in some viruses and uncleaved in others, and since several reports demonstrate that gB cleavage is dispensable for virus entry, it remains difficult to envisage a common role for different gBs in the herpes virus fusion machinery. As hypothesized in a previous report[13] in which mimetic peptides were used to demonstrate possible intramolecular (gB oligomers) and intermolecular (gB–gH) interactions through heptad repeat regions, and as confirmed by the analysis of the HSV-1 gB structure,[22] gB might have characteristics in common with both class I and class II fusion proteins, and probably needs to cooperate with gH to give rise to a fully competent fusion complex.

It is also conceivable that the mechanism by which some virus proteins facilitate fusion is a complex process involving multiple regions of the protein.[11,35–37] These regions, either directly or indirectly, might interact with biological membranes, contributing to the viral envelope and cell membrane merging. The presence of a number of membranotropic domains within viral fusion glycoproteins has been recognized for a variety of viruses.[38,39] It has also been reported that HSV-1 gH contains four domains (amino acid residues 220–262, 381–420, 579–597 and 626–644) that can induce the fusion of liposomal membranes,[11] so we have extended these studies and investigated the properties of peptides derived from specific regions of gB. We selected BoHV-1 and HSV-1 as representatives of herpes viruses with cleaved and uncleaved gBs, and screened their amino acid sequences for regions of highly interfacial hydrophobicity, applying the hydrophobicity-at-interface scale proposed by Wimley and White.[40] Synthetic peptides corresponding to such regions were tested for their ability to induce the fusion of large unilamellar vesicles and to inhibit virus infection. We have also analysed the characteristics of three peptides derived from the central helical region of gB that have been postulated (on the basis of structural data) to be involved in trimer formation.

Results

Interfacial hydrophobicity analysis, helical propensity and identification of peptide sequences

In order to identify hydrophobic stretches with the potential to interact with target membranes in the sequence of gB, we used the hydrophobicity-at-interface algorithm proposed by Wimley and White.[40–41] The hydrophobicity-at-interface scale has previously been successfully used to detect putative membrane-interacting regions within sequences of several fusogenic proteins of other viruses.[42] The results of this analysis of HSV-1 and BoHV-1 gB are shown in Figure 1. For HSV-1 gB, the first peak at the N terminus corresponds to the signal peptide sequence. Four further significantly hydrophobic regions were also identified (corresponding to residues 168–186, 287–305, 441–459 and 632–650), as well as two domains of relatively lower hydrophobicity corresponding to residues 389–398 and 653–671. Finally, at the C terminus we identified a large hydrophobic peak corresponding to the transmembrane region of the glycoprotein.

A similar analysis of the sequence of BoHV-1 gB (Figure 1B) revealed the presence of only two significantly hydrophobic regions other than the N-terminal signal peptide sequence: the region toward the N terminus (residues 181–198) corresponds to region 168–186 of HSV-1 gB, and the domain toward the C terminus (amino acid residues 664–678) corresponds to HB632–650. All the other peaks showed significantly lower hydrophobicity.

Analysis of the sequence alignments of HSV-1 and BoHV-1 gB showed that only one hydrophobic domain is located toward the C terminus while the others are all located in the N-terminal portion of gB that is cleaved in the bovine virus. We also analysed the sequence of the N-terminal region of the membrane-bound cleaved form of BoHV-1 gB in further detail. Despite the absence of any significant hydrophobicity peak in this domain, we noted that a region located just after the cleavage site (residues 525–548) showed some homology to the fusion peptide of HIV gp41. A similar sequence was also present in HSV-1 gB (residues 491–514; Figure 2A).

We also analysed the locations of predicted hydrophobic regions in terms of the context of the crystal structure of HSV-1 gB[22] (Figure 3). The gB ectodomain is made up of three protomers, and each protomer coils around the others with a left-handed twist; multiple contacts between protomers through-

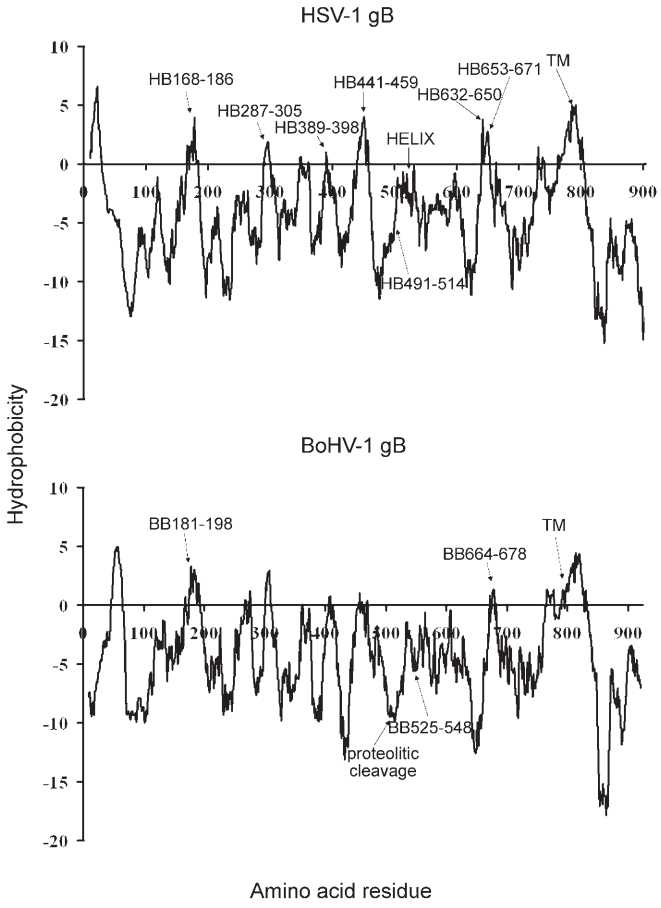

Figure 1. Hydrophobicity plots corresponding to the sequence of: A) the gB glycoprotein from HSV-1, and B) BoHV-1. The plots were elaborated by using the Wimley–White interfacial hydrophobicity scales for individual residues. The positions of the selected peptide are indicated.

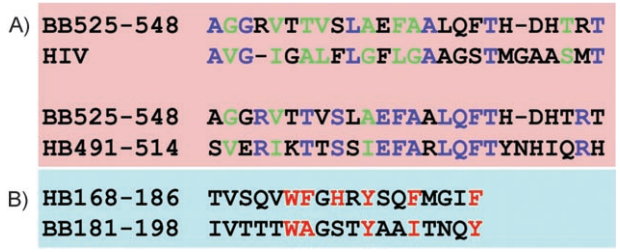

Figure 2. A) Sequence alignments between BoHV, HSV and HIV, showing the similarity between BB525–548 and the fusion peptide of HIV, and between BB525–548 and HB491–514. B) Sequence alignment between the putative fusion peptide of HSV-1 gB (HB168–186) and the corresponding sequence in BoHV-1 (BB181–198).

out the molecule contribute to trimer stability. Each protomer of gB can be divided into five distinct domains: I (base), II (middle), III (core), IV (crown) and V (arm). Domain I (Ile154 to Val363) is a β-sandwich composed of two nearly orthogonal β-sheets of four and three strands, with a long loop and short helix covering one opening of the β-sandwich. An insertion (Tyr165 to Ile272) between strands β4 and β11 creates a sub-

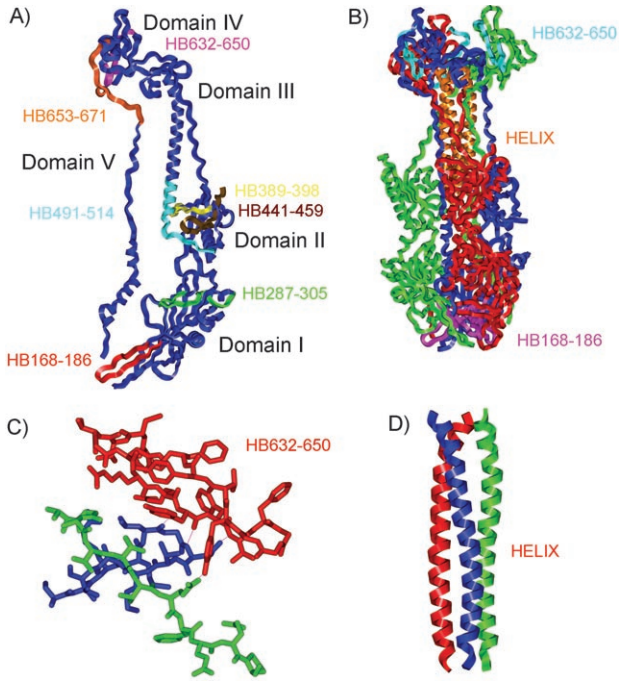

Figure 3. A) Three-dimensional structure of a single gB protomer; the domains corresponding to selected peptides are rendered in different colours. B) gB trimer; the three protomers are shown in different colours (green, blue and red) and the three most active peptides—HB168–186, HB632–650 and HELIX—are shown. C) Molecular details of the interactions between the peptide HB632–650 (red) and domains 120–130 (green) and 560–570 (blue) from a neighbouring monomer. D) Details of the interactions between domains corresponding to the HELIX peptide in the gB trimer.

domain at the base of the trimer, consisting of a four-stranded β-sheet (with three long and one short strand), the convex side of which is covered with an α-helix, a β-hairpin, and a short two-stranded β-sheet; the four-stranded β-sheet presents hydrophobic tips that have been proposed to be the putative fusion peptides of gB.[22,43] Peptides HB168–186 and HB287–305 are located in domain I; peptide HB168–186 is located in the insertion between strands β4 and β11 and corresponds to the hydrophobic tip that has been proposed to be the fusion peptide,[22,43] whilst peptide HB287–305 corresponds to the long loop covering one opening of the β-sandwich. The second hydrophobic tip that has been proposed to be a fusion peptide[22,43] does not correspond to a hydrophobicity peak and was not considered in this work.

Domain II comprises two discontinuous segments (Tyr142 to Asn153 and Cys364 to Thr459) and is characterized by the presence at its centre of a six-stranded β-barrel, with strand β5 substituted by an α-helix strand insert on the outer face of the barrel and with the entire domain I inserted between strands β3 and β17. Peptides HB389–398 and HB441–459 are located in domain II and partially interact with the helix domain.

Domain III, comprising three discontinuous segments (Pro117 to Pro133, Ser500 to Thr572, and Arg661 to Thr669), contains a long, 44-residue α-helix followed by a short helix and a small, four-strand mixed β-sheet. The long helix, together with the same helixes from the other protomers, forms the central coiled-coil (Figure 3 A and B). Peptides HB653–671 and

HB491–514 are located in domain III; in particular, peptide HB491–514 corresponds to the linker between domains II and III and to the N terminus of the long helix of domain III and, on the basis of our findings with this peptide and of the analysis of the three-dimensional structure we synthesized three additional peptides to include in this study (HELIX, C-HELIX and N-HELIX), corresponding to the long 44-residue α-helix and its shorter sequences (Figure 3D), while peptide HB653–671 is located in the outer β-strand of domain III, a region of the protein that contributes many of the essential contacts for gB trimerization.

Domain IV comprises two discontinuous segments (Ala111 to Cys116 and Cys573 to Ser660) linked by a disulfide bond. Peptide HB632–650 corresponds to a β-hairpin located in domain IV (Figure 3A–C). Domain V (Phe670 to Ala725) stretches from top to bottom of the molecule as a long extension; residues in this segment have no contact with the rest of the polypeptide chain of the same protomer but rather fit into the groove between the core domains of the other two protomers, probably reinforcing the trimer interactions. None of the selected peptides falls in this domain.

Fusogenic ability of gB-derived peptides

The fusogenic activity of the peptides was determined by their ability to cause lipid mixing of large unilamellar vesicles (LUVs) composed of PC/Chol (1:1). A population of LUVs labelled with both NBD-PE and Rho-PE was mixed with a population of unlabelled LUVs in the presence of increasing concentrations of peptides. Fusion between the labelled and unlabeled vesicles caused by the peptides results in dilution of the labelled lipids and therefore in reduced energy transfer between NBD-PE and Rho-PE. This change can be visualized as an increase in NBD fluorescence.

The dependence of both the extent and the kinetics of lipid mixing on the peptide to lipid molar ratio were analysed. Increasing amounts of each peptide were added to fixed amounts of vesicles and the percentage of lipid mixing as a function of the peptide-to-lipid molar ratio was calculated. No fusion was detected with scrambled peptides or 10% DMSO (data not shown). Figure 4A and B show the results of lipid mixing assays with PC/Chol-containing vesicles. HB287–305, HB389–398, HB441–459 and HB653–671 are unable to induce lipid mixing under these conditions (Figure 4A). However, we observed significant vesicle fusion in the presence of HB168–186 and HB632–650. HB168–186 was the most effective of the N-terminally located peptides at inducing lipid mixing, while HB632–650—located toward the C terminus—was even more effective. It was interesting to note that HB632–650 and HB653–671 precede the pre-transmembrane domain of gB, consistently with a common feature of fusion proteins, namely the involvement of the carboxy-terminal region of the ectodomain in fusion. Since the two most active HSV-1 gB-derived peptides were HB168–186 and HB632–650, we determined whether the analogous regions of BoHV-1 gB shared this property, and we found that the analogue of HB168–186—namely BB181–198—induced low levels of fusion, while BB644–678 showed a similar activity to HB632–650 (Figure 4B). We also found that BB525–548 and HB491–514, which are the two sequences selected on the basis only of a minor alignment to the HIV fusion peptide and located after the proteolytic cleavage site in BoHV-1 gB, both induce significant fusion of liposomes, comparable to the activity of HB168–186 (Figure 4B).

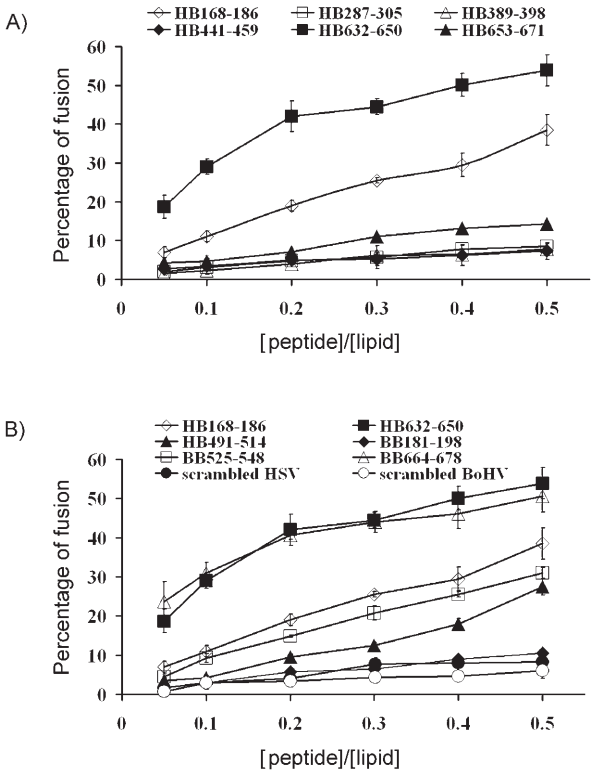

Figure 4. Peptide-promoted membrane fusion of PC/Chol (1:1) LUVs as determined by lipid mixing; peptide aliquots were added to LUVs (0.1 mM), containing NBD (0.6%) and Rho (0.6%). The increase in the fluorescence was measured 15 min after the addition of peptide aliquots; reduced Triton-X-100 (0.05%, *v/v*) was referred to as 100% of fusion. Dose dependence of lipid mixing is reported. A) HSV-1-derived peptides, B) active HSV-1-derived peptides and BoHV-1-derived peptides.

Effect of peptides on virus infectivity

All the peptides were also screened for their ability to inhibit plaque formation. To confirm that these peptides did not exert toxic effect on cells, monolayers were exposed to a range of concentrations (10, 50, 100, 250 and 500 μM) of each peptide for 24 h, and cell viability was assayed by an LDH assay. No statistical difference was observed between the viability of control (untreated) cells and that of cells exposed to the peptides (data not shown).

To test whether peptides derived from gB could affect HSV infectivity, Vero cells were infected with HSV-1 in the presence or absence of each peptide under a range of different conditions as described in the Experimental Section. Experiments were carried out to identify which step in the entry process was inhibited by gB-derived peptides. These results are shown in Figure 5. We chose a peptide concentration of 250 μM, as

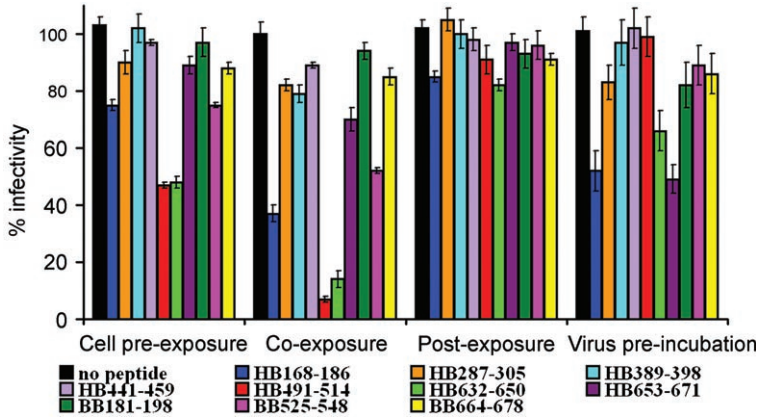

Figure 5. Cells were exposed to peptides at concentrations of 250 μM either prior to infection (Cells pre-exposure), during attachment and entry (Co-exposure) or after virus penetration (Post-exposure), or alternatively, the virus was pre-incubated with peptides for 1 h at 37 °C before addition to the cells (Virus pre-incubation). For all treatments, non-penetrated viruses were inactivated with low-pH citrate buffer after the 45 min incubation with cells at 37 °C. The cells were then incubated for 48 h at 37 °C in DMEM supplemented with CMC and plaque numbers were scored. Experiments were performed in triplicate, and the percentages of inhibition were calculated with respect to no-peptide control experiments. Error bars represent standard deviations.

inhibition of herpes virus infection with glycoprotein-derived peptides has been successfully demonstrated at this concentration,[13,14,44] and compared the effect of four different methods of exposure of the cells and/or virus to peptide. All active peptides only inhibited HSV infection prior to virus penetration into cells. None of the peptides was active in the post-exposure treatment, in which cells were infected for 45 min and peptides were then added to the cultures. HB168–186, HB491–514 and HB632–650 were all active in the co-exposure experiment and also inhibited infection to a minor extent if either the virus or the cells were pre-incubated with peptide. Peptides corresponding to sequences from BoHV-1 gB did not significantly inhibit HSV-1 infectivity.

Peptides HB168–186, HB491–514 and HB632–650 showed dose-dependent inhibition of HSV infectivity when present on the cell monolayers together with the virus inoculum for the 45 min period prior to low pH treatment (Figure 6 A). The most active peptides were HB632–650 and HB491–514; in fact, approximately 90% inhibition was observed at peptide concentrations of 250 μM (HB632–650: $IC_{50}=59$ μM; HB491–514: $IC_{50}=21$ μM). Figure 6 B also shows the results of a dose response co-exposure experiment in which MDBK cell monolayers were treated with BoHV-1-derived peptides and infected with the bovine virus (BB664–678: $IC_{50}=125$ μM; BB525–548: $IC_{50}=65$ μM).

To determine the specificity of the inhibitory effect of HSV-1 gB-derived peptides and to analyse the inhibitory activity of the BoHV-1 gB-based peptides, we tested all the active HSV-1 gB peptides and the BoHV-1 gB-derived peptides for their ability to inhibit the infectivity both of the homologous and of the heterologous virus (Figure 7). While HB168–186, HB632–650 and BB664–678 only inhibited infection by the viruses from which their gB sequences were derived, it was interesting to note that the two peptides HB491–514 and BB525–548, which had been identified on the basis of sequence alignment with the HIV fusion peptide, were active against both HSV-1 and BoHV-1. HB491–514 reduced HSV-1 infectivity by almost 90% and BoHV-1 infectivity by about 70% (at 250 μM), and BB525–548 reduced BoHV-1 infectivity by about 80% and HSV-1 infectivity by approximately 50%.

Since HB491–514 partially overlaps the central helix that, from structural data, constitutes the central core of the coiled coils of the gB trimer, we hypothesized that the inhibitory activity of HB491–514 could be due to an interaction of this peptide with the helix, thereby disrupting trimer formation. We therefore generated three additional peptides derived from this region: HELIX (corresponding to the entire helix), N-HELIX and C-HELIX (the former comprising the N terminus of the HELIX peptide and the latter comprising its C terminus). As shown in Figure 8, all three of these peptides were able to inhibit HSV1 infectivity, but the peptide corresponding to the full-length helix was by far the most effective.

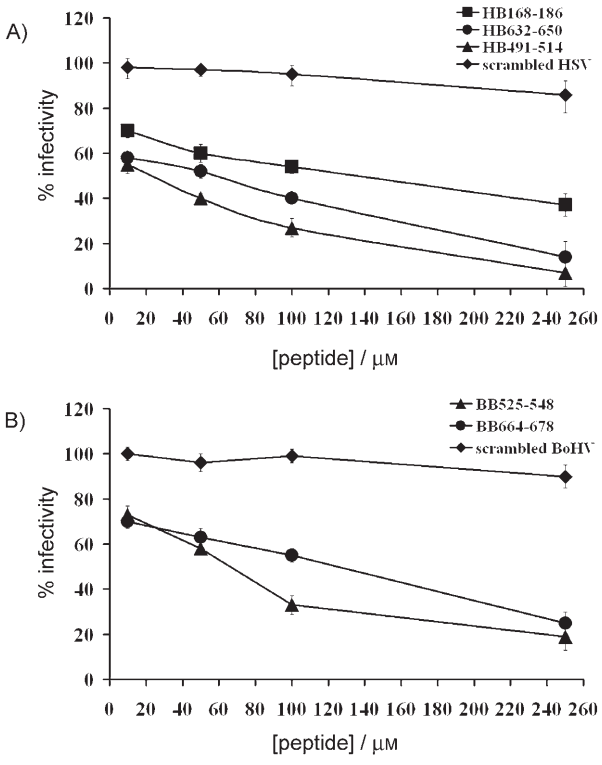

Figure 6. Cells were incubated with increasing concentrations of the peptides (10, 50, 100, 250 μM) in the presence of the viral inoculum for 45 min at 37 °C. Nonpenetrated virus was inactivated, and cells were incubated for 48 h at 37 °C in DMEM supplemented with CMC. Plaque numbers were scored, and the percentage of inhibition was calculated with respect to no-peptide control experiments. Data are reported in triplicate, and error bars represent standard deviations. A) Peptides from HSV-1: HB168–186, HB632–650, HB491–514. B) Peptides from BoHV-1: BB525–548, BB664–678.

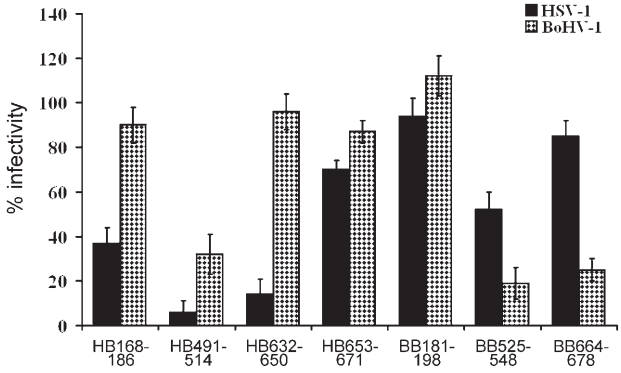

Figure 7. Active HSV-1- and BoHV-1-derived peptides' inhibition of both bovine and human viruses. Cells (Vero and MDBK cells) were exposed to peptides at concentrations of 250 μM during attachment and entry (Coexposure). Experiments were performed in triplicate, and the percentages of inhibition were calculated with respect to no-peptide control experiments. Error bars represent standard deviations.

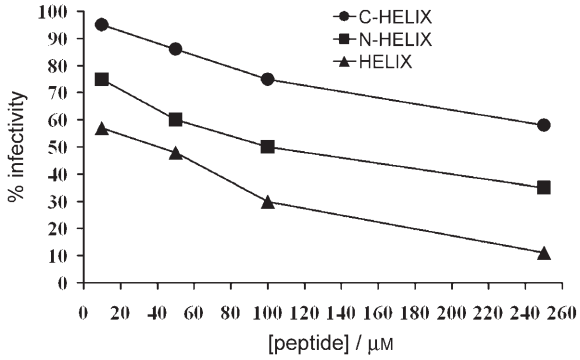

Figure 8. Vero cells were incubated with increasing concentrations of the peptides HELIX, N-HELIX and C-HELIX (10, 50, 100, 250 μM) in the presence of the viral inoculum for 45 min at 37 °C. Nonpenetrated virus was inactivated, and cells were incubated for 48 h at 37 °C in DMEM supplemented with CMC. Plaque numbers were scored, and the percentage of inhibition was calculated with respect to no-peptide control experiments. Data are reported in triplicate, and error bars represent standard deviations.

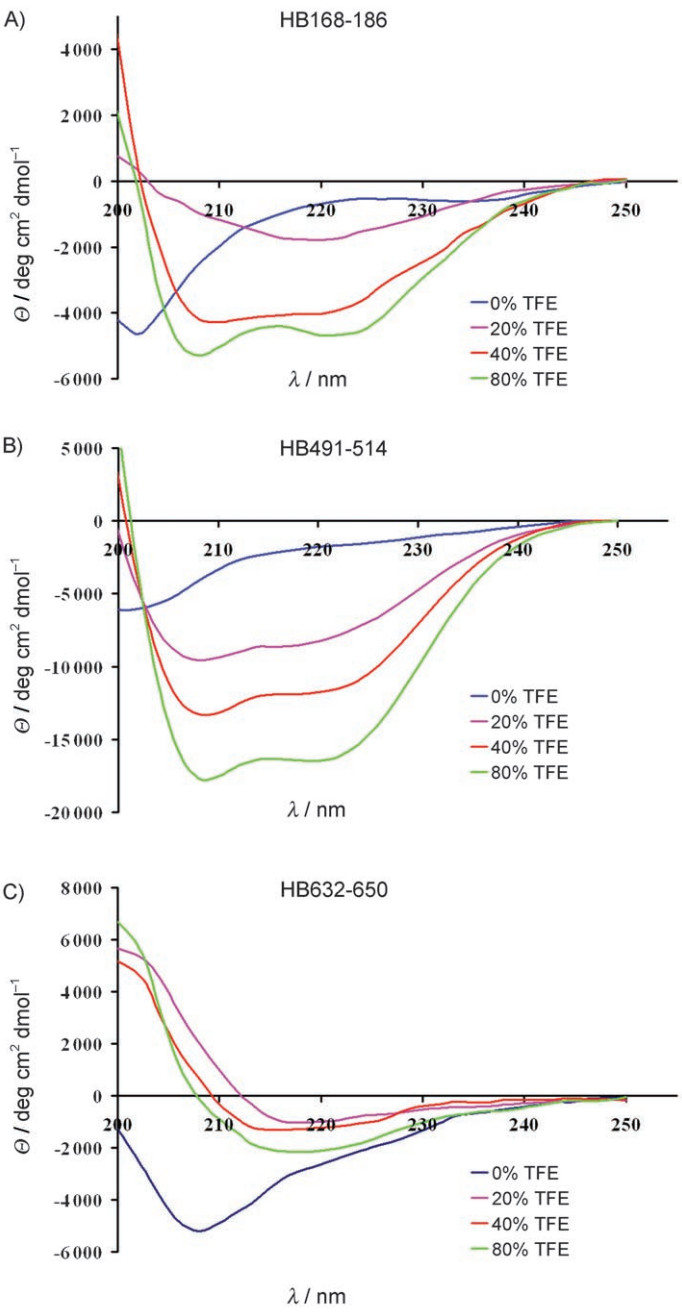

Figure 9. Circular dichroism spectra of peptides HB168–186, HB491–514 and HB632–650 (10 μM) at different percentages of TFE.

Secondary structures of synthetic peptides

Since the structural conformations of peptides have been shown in many cases to correlate with fusogenic and/or inhibition activity, the secondary structures of those gB peptides that were active in fusion and/or inhibition experiments were determined by CD spectroscopy as measured in water and TFE.

The CD spectra in buffer solution indicated random coil conformations for the peptides HB168–186, HB491–514, HB632–650, BB 525–548 and BB664–678 (Figures 9 and 10).

A decrease in peptide environmental polarity occurs when a peptide is transferred from water to a membrane interface, and the effect of polarity on peptide conformation can be studied by using aqueous mixtures of TFE. In the presence of TFE, peptides HB168–186, HB632–650 and BB664–678 all showed spectra that indicated the presence of extended structures with minima at approximately 218 nm. Spectra of the peptide BB664–678, however, were consistent with an increase in ellipticity in low-polarity solvent; in fact, increasing amounts of TFE induced stabilization of α-helical structures, characterized by the presence of minima at 208 and 222 nm, with approximately 20% helical content at 80% TFE. At low percentages of TFE a β-form can exist if a segment has β-forming potential, but excess TFE usually disrupts the β-form and may convert it into a helix if the segment also has helix-forming potential. Spectra were also collected in SUVs, and the results confirmed the ability of peptides HB168–186, HB491–514 and

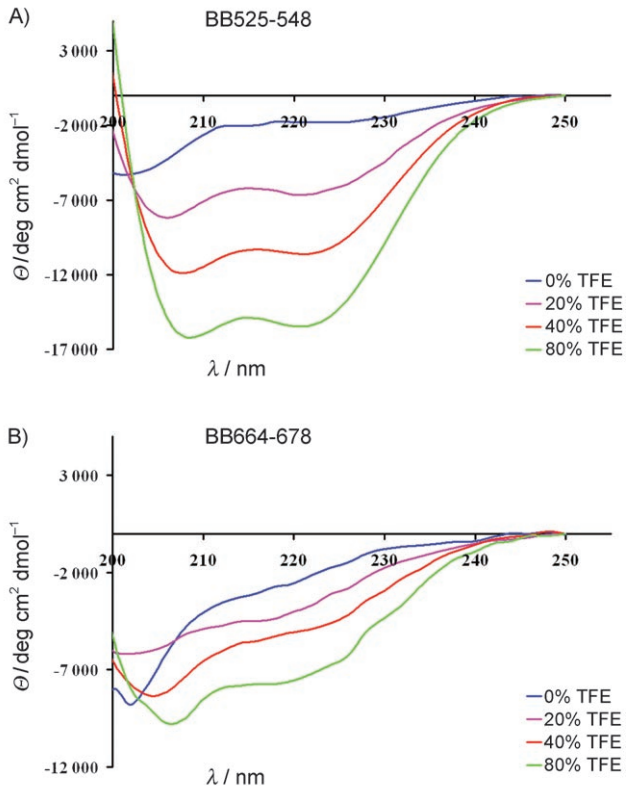

Figure 10. Circular dichroism spectra of peptides BB525–548 and BB664–678 (10 μM) at different percentages of TFE.

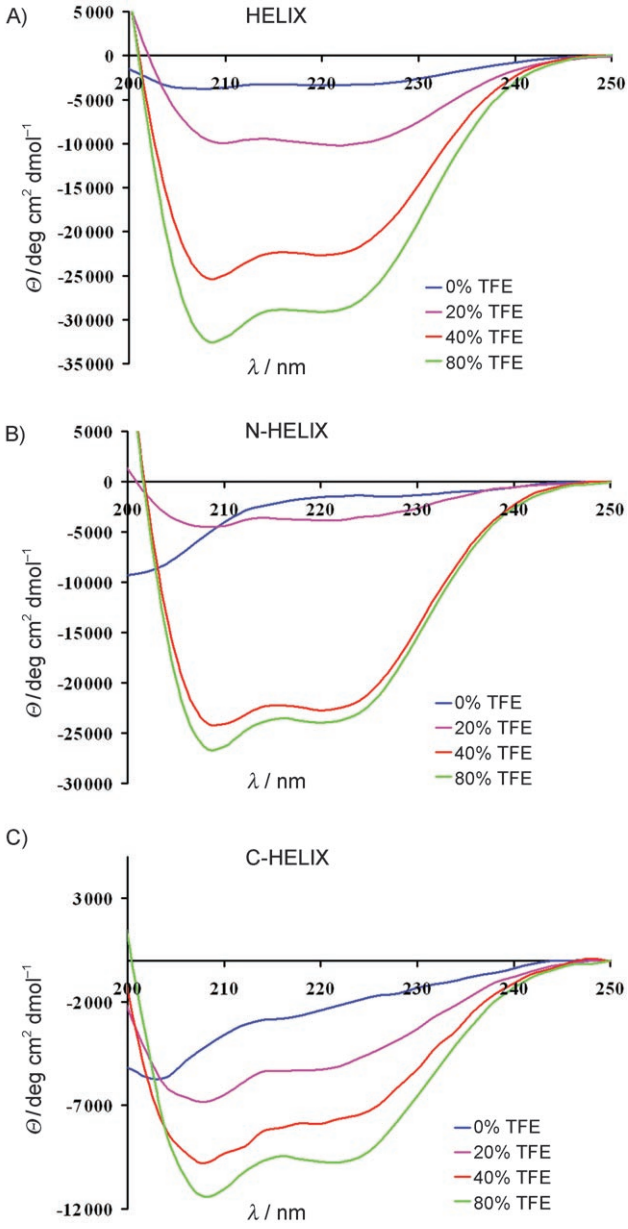

Figure 11. Circular dichroism spectra of peptides HELIX, N-HELIX and C-HELIX (10 μM) at different percentages of TFE.

BB525–548 to produce α-helices in membrane mimetic environments (data not shown).

Figures 9 and 10 show the CD spectra of the peptides HB491–514 and BB525–548; each peptide shows a typical random coil CD spectrum in buffer, whilst in contrast, high percentages of TFE induce approximately 45% helix content in each peptide.

Finally, the spectra of peptides HELIX, N-HELIX and C-HELIX were analysed (Figure 11). While peptide HELIX was able to adopt an α-helical conformation in buffer (approximately 10% helix), the other two peptides each showed a random coil conformation in buffer. Moreover, the three peptides were all able to adopt helical conformations at high percentages of TFE: 77%, 66% and 28% helical content for HELIX, N-HELIX and C-HELIX, respectively, at 80% TFE.

Discussion

Enveloped viruses are surrounded by membranes and infect cells by fusion of the viral membrane and a cellular membrane. The critical early events in viral infection are mediated by envelope glycoproteins and in many cases a viral fusion peptide is involved in the first steps of membrane fusion, penetrating the target membrane and initiating fusion of the viral envelope with the cell membranes. Recent studies have indicated that additional regions of viral fusion proteins, in combination with the fusion peptide, may also participate in conjunction with the fusion peptide in facilitating the apposition of the viral and cellular membranes. Such membranotropic segments would form a continuous track of membrane-interacting surfaces along the structure of the protein complex, providing a low-energy passageway for viral–cellular membrane fusion. Protein-mediated viral fusion is therefore a complex process in which multiple regions from viral fusion proteins may interact to lead to the destabilization and fusion of membranes. Several structural conformational changes induced by a complex series of protein–protein and protein–phospholipid interactions occur in fusion proteins. It is now evident that several domains are essential for membrane fusion and that peptides involved in the fusion mechanism might thus interfere with the intra-

molecular interactions between the several domains and result in the inhibition of virus entry.

The entry of herpes viruses requires a multicomponent fusion system, and HSV requires four glycoproteins—gD, gB and gH/gL—in order to accomplish this process. The roles of gH and gB remain elusive, but recent progress towards an understanding of their function includes the determination of the three-dimensional structure of gB and the identification of potentially fusogenic domains in gH.

It has been proposed that HSV-1 gH is directly involved in the interaction of the virus envelope and host cell membranes and that four regions (gH220–262, gH381–420, gH579–597 and gH626–644) might act in a synergistic way to facilitate such interactions;[11] moreover, two heptad repeat domains have been identified in gH (HR-1 and HR-2), whilst synthetic peptides mimicking these domains inhibit virus infection and form stable complexes with higher α-helical contents than those of the two peptides alone.[13,14] The recent determination of the crystal structure of HSV-1 gB[22] represents a major advance in our understanding of herpes virus entry, revealing that gB shares characteristic with both class I and class II fusion proteins of other viruses. From these findings it is conceivable to envisage a scenario in which gH and gB cooperate with each other during the fusion process. Moreover, it has been proposed that gH and gB are likely to function sequentially to promote membrane fusion, with gH initiating lipid mixing to lead to a hemifusion intermediate and gB stabilizing and expanding the pore to allow complete fusion.[10]

This study suggests that the region encompassing residues 168–186 and 632–671 of HSV-1 gB corresponds to membrane-partitioning domains with the ability to perturb the integrity of PC/cholesterol-containing phospholipid bilayers, and might constitute functional elements of HSV-1 gB involved in the promotion of the membrane destabilization required for fusion. The two domains are located on either side of the position of the post-translational cleavage site that is present in some herpes virus gB homologues.

In lipid mixing experiments (Figure 4), we observed significant vesicle fusion in the presence of HB168–186 and HB632–650. The analysis of the secondary structures of the same peptides revealed their ability to adopt different conformations according to the environment.

The structural plasticity of membrane-associated viral fusion peptides has been observed for several viruses, and it is known that fusion peptides can exist in helical and nonhelical forms. Moreover, it is interesting to evaluate their location in the protein structure of gB, as Heldwein et al.[22] propose that the putative fusion peptide of gB is located at the tip of domain I. Of the two loops that were proposed to be the fusion peptide, only one corresponds to a peak of interfacial hydrophobicity, and the peptide mimicking this loop domain is HB168–186 and is active in fusion experiments. Peptide HB632–650 is located on the other side of the protein in the outer β-strand of domain III, which contributes many of the essential trimer contacts; in fact, several hydrogen bonds and van der Waals interactions between the 632–650 fragment of one monomer and the domains 120–130 and 560–570 of a neighbouring monomer are present in the crystal structure (Figure 3C). Moreover, this peptide has the features of a fusion peptide—the presence of an extended structure in TFE and a high content of aromatic residues—and is efficient at inducing the fusion of liposomes.

The corresponding peptides derived from BoHV-1 gB were also tested for their ability to fuse liposomes, and we found that whereas BB664–678 was as efficient in these assays as its HSV-1 gB counterpart (HB632–650), BB181–198 had a low fusogenic capacity. Sequence comparison of HB168–186 and BB181–198 (Figure 2B) shows that two phenylalanine residues in HB168–186 are substituted by non-aromatic residues in BB181–198, and this may account for the inability of BB181–198 to induce liposome fusion. Moreover, mutations of residues Trp174 and Tyr179 seriously impair HSV-1 gB function, further confirming the fundamental role played by aromatic residues during insertion into the target membrane.

This result is highly intriguing, since the uncleaved HSV-1 gB shows a potential fusion peptide in Domain I, as identified by analysis of its crystallographic structure,[22] but retains a stretch of amino acids with fusion potential in the region downstream of the location of the furin cleavage site of other herpes virus gB molecules, implying functional conservation regardless of proteolytic cleavage. Therefore, cleaved and uncleaved gB proteins showed several membrane interacting motifs both at the N terminus and after the proteolytic cleavage site, indicating a possibly divergent mechanism of fusion based on functionally conserved hydrophobic regions.

Peptides HB491–514 and BB525–548 each showed small but significant activity in both fusion experiments and infectivity inhibition assays. An analysis of the locations of these regions within the three-dimensional structure of gB indicates that they corresponded partially to the long helix in domain III. The long 44-residue α-helix and its trimeric counterparts form the central coiled-coil, and the potential function of this domain was further analysed with the peptides HELIX, N-HELIX and C-HELIX. Infectivity inhibition experiments showed that HELIX is an active inhibitor of HSV-1 fusion and we speculate that its activity might be due to a possible trimer destabilization.

These results support the view that gH and gB are both directly involved in membrane fusion; both molecules contain multiple domains that are capable of interacting with membranes, and peptides from specific regions of both proteins can inhibit virus infection. A recent report also suggested that multiple domains are critical for gB function, and that different gB functional regions (analysed by monoclonal antibodies) may be involved in HSV entry.[45]

Further characterization of such domains is likely to shed further light on the complex mechanism of herpes virus glycoprotein-mediated membrane fusion.

Experimental Section

Materials: Fluorenylmethoxycarbonyl-protected (Fmoc-protected) amino acids were purchased from INBIOS (Pozzuoli, NA, Italy), NovaSyn TGA resin was purchased from Nova Biochem (Darmstadt, Germany). The reagents (piperidine, pyridine) for the solid-phase

peptide synthesis were purchased from Fluka (Sigma–Aldrich, Milano, Italy), trifluoroacetic acid (TFA) and acetic anhydride were from Applied Biosystems (Foster City, CA, USA), and H_2O, DMF and CH_3CN were supplied by LAB-SCAN (Dublin, Ireland). Egg phosphatidylcholine (PC), cholesterol (Chol) and the fluorescent probes *N*-(7-nitro-benz-2-oxa-1,3-diazol-4-yl)phosphatidylethanolamine (N-NBD-PE) and *N*-(lissamine-rhodamine-B-sulfonyl)phosphatidylethanolamine (N-Rh-PE) were purchased from Avanti Polar Lipids (Birmingham, AL). Triton-X100 was obtained from Sigma. All other reagents were of analytical grade.

Proteomics computational methods: Domains with significant propensity to form transmembrane (TM) helices were identified with Tmpred (ExPaSy, Swiss Institute of Bioinformatics) and Membrane Protein eXplorer (MpeX, Stephen White laboratory, http://blanco.biomol.uci.edu/mpex). Tmpred is based on a statistical analysis of Tmbase, a database of naturally occurring TM glycoproteins, while MpeX detection of membrane-spanning sequences is based on experimentally determined hydrophobicity scales.[40,41] Sequences with a propensity to partition into the lipid bilayer were also identified by MpeX by use of interfacial settings, with mean values for a window of 11 amino acids. Scrambled versions of the most active peptides of the human and bovine virus were designed with consideration of the hydrophobicity, the helix propensity etc. Alignments were performed with Blast and ClustalW. The gB sequences used were taken from the SWISS-Prot database, with accession numbers P10211 for human gB and P17471 for bovine gB. Coordinates for gB were obtained from the Protein Data Bank (PDB) with accession number 2gum.

Peptide synthesis: Peptides were synthesized by standard solid-phase 9-fluorenylmethoxycarbonyl (Fmoc) methods as previously reported.[11] All purified peptides were obtained with good yields (30–40%). Table 1 shows the sequences of all the synthesized peptides. Peptide stock solutions were prepared in dimethyl sulfoxide (DMSO, 2%).

Liposome preparation: Large unilamellar vesicles (LUVs) consisting of PC/Chol (1:1) with different amounts of Rho-PE and NBD-PE were prepared by the extrusion method of Hope et al.[46] in HEPES (5 mM), NaCl (100 mM), pH 7.4. Briefly, lipids were dried from chloroform solution with a nitrogen gas stream and liophilized overnight. For fluorescence experiments, dry lipid films were suspended in buffer by vortexing to produce large unilamellar vesicles. The lipid suspension was freeze-thawed eight times and then extruded 20 times through polycarbonate membranes with 0.1 μm diameter pores.

Table 1. Peptide sequences.

Peptides	Protein fragment	Sequences
HSV-1 gB		
HB168–186	168–186	VTVSQVWFGHRYSQFMGIF
HB287–305	287–305	FVLATGDFVYMSPFYGYRE
HB389–398	389–398	YGGSFRFSSDAISTTFTTN
HB441–459	441–459	YYLANGGFLIAYQPLLSNT
HB491–514	491–514	SVERIKTTSSIEFARLQFTYNHIQ
HB632–650	632–650	PCTVGHRRYFTFGGGYVYF
HB653–671	653–671	YAYSHQLSRADITTVSTFI
scrambled HSV	632–650	FVRGHTGFVYCYGYTGFPR
HELIX	500–544	SIEFARLQFTYNHIQRHVNDMLGRVAIAW-CELQNHELTLWNEARK
N-HELIX	500-523	SIEFARLQFTYNHIQRHVNDMLGR
C-HELIX	524-544	VAIAWCELQNHELTLWNEARK
BoHV-1 gB		
BB181–198	181–198	IVTTTWAGSTYAAITNQY
BB525–548	525–548	AGGRVTTVSLAEFAALQFTHDHTR
BB664–678	664–678	ANHKRYFRFGADYVY
scrambled BoHV	664–678	GRYKFYARFDHNVYA

Lipid mixing assay: Membrane lipid mixing was monitored by the resonance energy transfer (RET) assay reported by Struck et al.[47] The assay is based on the dilution of the NBD-PE (donor) and Rho-PE (acceptor) groups. Dilution due to membrane mixing results in an increase in NBD-PE fluorescence. We thus monitored the change in donor emission as aliquots of peptides were added to vesicles. Vesicles containing each probe (0.6 mol%) were mixed with unlabelled vesicles at a 1:4 ratio (final lipid concentration 0.1 mM). Small volumes of peptides in dimethylsulfoxide (DMSO) were added; the final concentration of DMSO was no higher than 2%. The NBD emission at 530 nm was followed with the excitation wavelength set at 465 nm. A cut-off filter at 515 nm was used between the sample and the emission monochromator to avoid scattering interferences. The fluorescence scale was calibrated such that the zero level corresponded to the initial residual fluorescence of the labelled vesicles, and the 100% value corresponding to complete mixing of all lipids in the system was set by the fluorescence intensity of vesicles upon the addition of Triton X-100 (0.05% *v/v*) at the same total lipid concentrations of the fusion assay. All fluorescence measurements were conducted in PC/Chol (1:1) LUVs; lipid mixing experiments were repeated at least three times and results were averaged. Control experiments were performed with scrambled peptides and DMSO.

Virus entry assays: Vero cells were grown in Dulbecco's modified Eagle's medium (DMEM) supplemented with foetal calf serum (10%). HSV-1 carrying a *LacZ* gene driven by the CMV IE-1 promoter to express β-galactosidase was propagated as previously described.[1] BoHV-1 (Cooper strain; ATCC VR-864) was replicated in Madin–Darby bovine kidney (MDBK; ATCC CCl22) cells in minimum essential medium (MEM) supplemented with foetal bovine serum (FBS, 5%) at 35 °C under a humidified CO_2 (5%) atmosphere. Peptides were dissolved in DMEM without serum and used at a range of concentrations. All experiments were conducted in parallel with scrambled peptides and no-peptide controls.

To assess the effect of peptides on inhibition of HSV and/or BoHV-1 infectivity, four different ways of treating cell monolayers were performed:

1) For "virus pretreatment", virus (approximately 2×10^4 PFU) was incubated in the presence of different concentrations of peptides (10, 100, 250, 500 μM) for 45 min at 37 °C, and was then titrated on cell monolayers.
2) For "cell pre-treatment", cells were incubated with peptides (10, 100, 250, 500 μM) for 30 min at 4 °C. Peptides were removed, and cells were washed with phosphate-buffered saline. Following this treatment, the cells were infected with serial ten-fold dilutions of HSV-1 or BoHV-1.
3) For "co-treatment", the cells were incubated with increasing concentrations of the peptides (10, 100, 250, 500 μM) in the presence of serial dilutions of viral inoculum for 45 min at 37 °C.
4) For "post-treatment", cell monolayers were infected with virus for 45 min at 37 °C. A range of concentrations of peptides (10, 50, 100, 250, 500 μM) was then added to the inoculum, followed by a further 30 min incubation at 37 °C.

For all treatments, nonpenetrated viruses were inactivated with citrate buffer (pH 3.0) after the 45 min incubation at 37 °C. Monolayers were incubated for 48 h at 37 °C in DMEM supplemented with carboxymethylcellulose (CMC), fixed and stained with X-gal (5-bromo-4-chloro-3-indolyl-β-D-galactopyranoside), and plaque numbers were scored. Experiments were performed in triplicate and the percentage of inhibition was calculated with respect to no-peptide control experiments.

Toxicity: Peptide cytotoxicity was measured by a lactate dehydrogenase (LDH) assay and was carried out according to manufacturer's instructions with use of a cytotoxicity detection kit (Roche Diagnostic SpA., Milano, Italy).

Circular dichroism measurements: CD spectra were recorded with a Jasco J-715 spectropolarimeter in a 1.0 cm quartz cell at room temperature. The spectra are each an average of three consecutive scans from 260 to 195 nm, recorded with a band width of 3 nm, a time constant of 16 s and a scan rate of 10 nm min^{-1}. Spectra were recorded and corrected for the blank. Mean residues ellipticities (MREs) were calculated by use of the equation obsd/lcn, where obsd is the ellipticity measured in millidegrees, l is the length of the cell in centimetres, c is the peptide concentration in moles per litre, and n is the number of amino acid residues in the peptide. The percentage of helix was calculated from measurements of their mean residue ellipticity at 222 nm.[48] We used $[\theta]_{222}$ values of 0 and $-40\,000(1-2.5/n)$ deg cm^2 dmol^{-1} per amino acid residue for 0% and 100% helicity; n is the number of amino acid residues. Solutions of peptides (10 μM) were prepared in water and at various percentages of TFE.

Acknowledgements

We gratefully acknowledge support by the EU under contract no.QLK2-CT-2002-00810.

Keywords: circular dichroism · hydrophobicity · liposomes · synthetic peptides · virus entry

[1] A. Forrester, H. Farrell, G. Wilkinson, J. Kaye, N. Davis-Poynter, T. Minson, *J. Virol.* **1992**, *66*, 341–348.
[2] D. C. Johnson, M. W. Ligas, *J. Virol.* **1988**, *62*, 4605–4612.
[3] W. H. Cai, B. Gu, S. Person, *J. Virol.* **1988**, *62*, 2596–2604.
[4] A. Turner, B. Bruun, T. Minson, H. Browne, *J. Virol.* **1998**, *72*, 873–875.
[5] P. G. Spear, M. T. Shieh, B. C. Herold, D. WuDunn, T. I. Koshy, *Adv. Exp. Med. Biol.* **1992**, *313*, 341–353.
[6] R. I. Montgomery, M. S. Warner, B. J. Lum, P. G. Spear, *Cell* **1996**, *87*, 427–436.
[7] R. J. Geraghty, C. Krummenacher, G. H. Cohen, R. J. Eisenberg, P. G. Spear, *Science* **1998**, *280*, 1618–1620.
[8] A. Carfí, S. H. Willis, J. C. Whitbeck, C. Krummenacher, G. H. Cohen, R. J. Eisenberg, D. C. Wiley, *Mol. Cell* **2001**, *8*, 169–179.
[9] C. Krummenacher, V. M. Supekar, J. C. Whitbeck, E. Lazear, S. A. Connolly, R. J. Eisenberg, G. Cohen, D. C. Wiley, A. Carfi, *EMBO J.* **2005**, *24*, 4144–4153.
[10] R. P. Subramanian, R. J. Geraghty, *Proc. Natl. Acad. Sci. USA* **2007**, *104*, 2903–2908.
[11] S. Galdiero, A. Falanga, M. Vitiello, H. Browne, C. Pedone, M. Galdiero, *J. Biol. Chem.* **2005**, *280*, 28632–28643.
[12] T. Gianni, P. L. Martelli, R. Casadio, G. Campadelli-Fiume, *J. Virol.* **2005**, *79*, 2931–2940.
[13] S. Galdiero, M. Vitiello, M. D'Isanto, A. Falanga, C. Collins, K. Raieta, C. Pedone, H. Browne, M. Galdiero, *J. Gen. Virol.* **2006**, *87*, 1085–1097.
[14] T. Gianni, L. Menotti, G. Campadelli-Fiume, *J. Virol.* **2005**, *79*, 7042–7049.
[15] V. C. Bond, S. Person, S. C. Warner, *J. Gen. Virol.* **1982**, *61*, 245–254.
[16] N. DeLuca, D. J. Bzik, V. C. Bond, S. Person, W. Snipes, *Virology* **1982**, *122*, 411–423.
[17] P. J. Gage, M. Levine, J. C. Glorioso, *J. Virol.* **1993**, *67*, 2191–2201.
[18] L. Pereira, *Infect. Agents Dis.* **1994**, *3*, 9–28.
[19] D. J. Bzik, B. A. Fox, N. A. DeLuca, S. Person, *Virology* **1984**, *137*, 185–190.
[20] W. Z. Cai, S. Person, C. DebRoy, B. H. Gu, *J. Mol. Biol.* **1988**, *201*, 575–588.
[21] L. Claesson-Welsh, P. G. Spear, *J. Virol.* **1987**, *61*, 1–7.
[22] E. E. Heldwein, H. Lou, F. C. Bender, G. H. Cohen, R. J. Eisenberg, S. C. Harrison, *Science* **2006**, *313*, 217–220.
[23] W. J. Britt, L. G. Vugler, *J. Virol.* **1989**, *63*, 403–410.
[24] L. C. Loh, *Virology* **1991**, *180*, 239–250.
[25] D. M. Meredith, J. M. Stocks, G. R. Whittaker, I. W. Halliburton, B. W. Snowden, R. A. Killington, *J. Gen. Virol.* **1989**, *70*, 1161–1172.
[26] L. J. Ross, M. Sanderson, S. D. Scott, M. M. Binns, T. Doel, B. Milne, *J. Gen. Virol.* **1989**, *70*, 1789–1804.
[27] D. C. Sullivan, G. P. Allen, D. J. O'Callaghan, *Virology* **1989**, *173*, 638–646.
[28] S. van Drunen Littel-van den Hurk, L. A. Babiuk, *J. Virol.* **1986**, *59*, 401–410.
[29] M. Vey, W. Schafer, B. Reis, R. Ohuchi, W. Britt, W. Garten, H. D. Klenk, K. Radsak, *Virology* **1995**, *206*, 746–749.
[30] M. Gong, T. Ooka, T. Matsuo, E. Kieff, *J. Virol.* **1987**, *61*, 499–508.
[31] L. Claesson-Welsh, P. G. Spear, *J. Virol.* **1986**, *60*, 803–806.
[32] A. Kopp, E. Blewett, V. Misra, T. C. Mettenleiter, *J. Virol.* **1994**, *68*, 1667–1674.
[33] T. C. Mettenleiter, P. G. Spear, *J. Virol.* **1994**, *68*, 500–504.
[34] T. Strive, E. Borst, M. Messerle, K. Radsak, *J. Virol.* **2002**, *76*, 1252–1264.
[35] R. M. Epand, *Biochim. Biophys. Acta Biomembr.* **2003**, *1614*, 116–121.
[36] S. G. Peisajovich, Y. Shai, *Biochim. Biophys. Acta Biomembr.* **2003**, *1614*, 122–129.
[37] S. Galdiero, A. Falanga, M. Vitiello, M. D'Isanto, C. Collins, V. Orrei, H. Browne, C. Pedone, M. Galdiero, *ChemBioChem* **2007**, *8*, 885–895.
[38] M. R. Moreno, M. Giudici, J. Villalain, *Biochim. Biophys. Acta Biomembr.* **2006**, *1758*, 111–123.
[39] A. J. Perez-Berna, M. R. Moreno, J. Guillen, A. Bernabeu, J. Villalain, *Biochemistry* **2006**, *45*, 3755–3768.
[40] W. C. Wimley, S. H. White, *Nat. Struct. Biol.* **1996**, *3*, 842–848.
[41] S. H. White, W. C. Wimley, *Annu. Rev. Biophys. Biomol. Struct.* **1999**, *28*, 319–365.
[42] T. Suarez, W. R. Gallaher, A. Agirre, F. M. Goni,, J. L. Nieva, *J. Virol.* **2000**, *74*, 8038–8047.
[43] B. P. Hannah. , E. E. Heldwein, F. C. Bender, G. H. Cohen, R. J. Eisenberg, *J. Virol.* **2007**, *81*, 4858–4865.
[44] M. Lopper, T. Compton, *J. Virol.* **2004**, *78*, 8333–8341.
[45] F. C. Bender, S. Minu, E. E. Heldwein, M. Ponce de Leon, E. Bilman, H. Lou, J. C. Whitbeck, R. J. Eisenberg, G. H. Cohen, *J. Virol.* **2007**, *81*, 3827–3841.
[46] M. J. Hope, M. B. Bally, G. Webb, P. R. Cullis, *Biochim. Biophys. Acta Biomembr.* **1985**, *812*, 55–65.
[47] D. K. Struck, D. Hoekstra, R. E. Pagano, *Biochemistry* **1981**, *20*, 4093–4099.
[48] A. Chakrabartty, T. Kortemme, R. L. Baldwin, *Protein Sci.* **1994**, *3*, 843–852.

Received: August 6, 2007
Published online on February 29, 2008

